Phys. Status Solidi B **250,** No. 10, 2080–2084 (2013) / **DOI** 10.1002/pssb.201384230

physica status solidi b
www.pss-b.com
basic solid state physics

# "Negative" diamagnetism of three-dimensional arrays of semiconductor nano-rings

**L. M. Thu[1,2], W. T. Chiu[1], and O. Voskoboynikov[*,1]**

[1] Department of Electronics Engineering, National Chiao Tung University, 1001 Ta Hsueh Rd., Hsinchu 30010, Taiwan, R.O.C.
[2] Department of Physics, Hanoi National University of Education, 136 Xuanthuy Road, Hanoi, Vietnam

Received 29 September 2010, revised 25 December 2012, accepted 12 August 2013
Published online 16 September 2013

**Keywords** diamagnetism, mapping method, nano-rings

[*] Corresponding author: e-mail vam@faculty.nctu.edu.tw, Phone: +886 3 5712121 ext: 54174, Fax: +886 37533722

We theoretically study the orbital diamagnetic response of three-dimensional arrays of embedded InAs/GaAs wobbled nano-rings. To simulate the rings' magnetic characteristics, we use the effective one band Hamiltonian (energy and position-dependent electron effective mass and Landé factor) and smooth three-dimensional confinement potential that is mapping the actual strain and material content inside the rings. First, we obtain the magnetic susceptibility of an individual nano-ring. Once it is achieved, using the Claussius–Mossotti relation we estimate the effective susceptibility of three-dimensional arrays of the rings. We show that conventionally diamagnetic InAs/GaAs ring structures under certain conditions can demonstrate the positive peak of the effective magnetic susceptibility of the arrays, that we call "negative"-diamagnetic response. The "negative"-diamagnetic (positive susceptibility) peak remains Lorentz-like shaped and gradually disappears when the rings' concentration in the arrays decreases.



**1 Introduction** Composite materials (metamaterials, artificially structured materials) offer a very promising direction of the future development of multiband and multifunctional nano-based semiconductor devices (see for instance [1–4] and others). Incorporating tuneable nano-sized components (nano-objects) into metamaterials or having nano-components with active and controllable inclusions one can achieve tuneable properties of the metamaterials, regardless of the origin of the modulation. Modern progress in semiconductor technologies makes it possible to fabricate semiconductor nano-objects of high quality and uniformity [5–10]. Those nano-objects are nano-sized semiconductor structures resembling atoms and their magnetic properties. On the other hand, nano-objects have the advantage of on-demand designed properties and they provide us with the possibility to manipulate and reconfigure electronic wave functions in three-dimensional space. To this end, a proper understanding of the connection between the quantum mechanics of coherent electronic states in isolated nano-objects and the collective electromagnetic response from arrays made from them is a prerequisite to develop principally new nano-structured metamaterials.

When looking for semiconductor nano-systems to realize unusual magnetic response, it is very instructive to recall the conventional classification of the magnetic materials. According to the general solid-state physics (see for instance [11–13]) the atomic magnetism arises from electron angular momentum (**L**) and spin (**S**). Magnetic field dependent terms in the atomic Hamiltonian can be presented as (magnetic field **B** is directed along $z$-axis):

$$\hat{H} = \mu_B(\hat{\boldsymbol{L}} + g_e\hat{\boldsymbol{S}})\cdot\boldsymbol{B} + \frac{e^2}{8m_e}B^2\sum_i(x_i^2 + y_i^2),$$
$$\hat{\boldsymbol{L}} = \textstyle\sum_i \hat{\boldsymbol{L}}_i; \quad \hat{\boldsymbol{S}} = \textstyle\sum_i \hat{\boldsymbol{S}}_i \tag{1}$$

where $\mu_B$ is the Bohr magneton, $m_e$ and $g_e$ stand for the free electron mass and Landé factor, $xy$-plane is chosen to be perpendicular to **B**, and $i$ enumerates electrons in the atom. Magnetic field as a perturbation leads to shifts of the electron energy level $E_{0n}$ (relating to the state wave function $|n\rangle$)

$$E_n \approx E_{0n} + \Delta E_n \tag{2}$$

where according to the general perturbation theory:

$$\Delta E_n = \mu_B \mathbf{B} \cdot \langle n|\hat{\boldsymbol{L}} + g_e \hat{\boldsymbol{S}}|n\rangle + \sum_{n' \neq n} \frac{\left|\langle n|\mu_B \mathbf{B} \cdot (\hat{\boldsymbol{L}} + g_e \hat{\boldsymbol{S}})|n'\rangle\right|^2}{E_n - E'_n} + \frac{e^2}{8m_e} B^2 \langle n| \sum_i (x_i^2 + y_i^2)|n\rangle. \quad (3)$$

A standard definition for the diamagnetic response assumes that in the ground state the atom has closed (filled) shells and $\hat{\boldsymbol{L}}|n\rangle = \hat{\boldsymbol{S}}|n\rangle = 0$, so only the last term in Eq. (3) represents the atomic magnetic response.

Magnetization inside materials $M$ (magnetic moment per unit volume) and magnetic polarizability $\chi$ of multi-atomic systems (treated as canonical ensembles) can be presented as the following functions of the magnetic field and temperature $T$:

$$M(B,T) = -N\frac{\partial F}{\partial B} = N\frac{\sum_n M_n(B) e^{-E_n/k_B T}}{\sum_n e^{-E_n/k_B T}}, \quad M_n(B) = -\frac{\partial E_n(B)}{\partial B}, \quad \chi = \frac{\partial M}{\partial B}, \quad (4)$$

where $F$ is Helmholtz free energy and $N$ stands for number of atoms per unit volume. According to the constitutive relations ($\mu_0$ is the vacuum magnetic permeability):

$$\mathbf{B} = \mu_0(\mathbf{H} + \mathbf{M}) \text{ and } \mathbf{B} = \mu \mathbf{H} \quad (5)$$

one can see that the material effective permeability is:

$$\mu = \frac{\mu_0}{1 - \mu_0 \chi} = \mu_0 \mu_{\text{eff}}, \quad \mu_{\text{eff}} \approx 1 + \mu_0 \chi = 1 + \chi_{\text{eff}}, \quad \{\text{if } |\mu_0 \chi| \ll 1\} \quad (6)$$

and the material is a paramagnet if $\chi_{\text{eff}} > 0$ and diamagnet if $\chi_{\text{eff}} < 0$. According to this consideration, the condition $\hat{\boldsymbol{L}}|n\rangle = \hat{\boldsymbol{S}}|n\rangle = 0$in Eq. (3) always lead to $\chi_{\text{eff}} < 0$. In addition the temperature behavior of the effective susceptibility $\chi_{\text{eff}}$ is very diverse: for paramagnets, it drops rapidly with the temperature growth, for diamagnets, it remains rather stable with the temperature change.

Considering the magnetic response of on-demand designed semiconductor nano-objects one can find properties those are very different from described above for atomic systems. As an example, we consider semiconductor nano-sized rings (NRs). Among semiconductor nano-objects, NRs have attracted much interest in the recent decade. They are non-simply connected nano-objects (unlike quantum dots) and this results the Aharonov–Bohm effect [14] followed by the oscillating persistent current [15] and orbital magnetization of the rings. Energy structures of electrons and holes as well as magneto-optical characteristics of those nano-rings

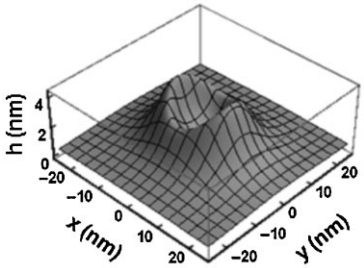


**Figure 1** Wobbled nano-ring.

were theoretically and experimentally investigated in details (see e.g. Refs. [15–19] and references therein). It was found that under certain conditions individual semiconductor InAs/GaAs nano-rings (designed from conventional diamagnetic semiconductor materials) can demonstrate positive differential magnetic susceptibility (DMS) or "negative"-diamagnetic response [15].

In this study, we theoretically consider diamagnetic properties of three-dimensional arrays of embedded InAs/GaAs wobbled nano-rings [15, 18] (see Fig. 1). We use a computational method (see e.g. Refs. [20–22] and references therein) which allows us to map realistic three-dimensional geometry, strain, and material composition of the rings (known from experiments) on three dimensional effective one-electronic band Hamiltonian (energy and position dependent electron effective mass approximation) for electrons confined in the rings when the external magnetic field $\mathbf{B}$ is applied in the system's growth directions.

Using solutions of the corresponding Schrödinger equation, we are able to simulate the magnetization and DMS of an isolated wobbled nano-ring [18, 20]. Having ready the DMS of an individual nano-ring we use the Claussius–Mossotti relation [13] to simulate the effective permeability and susceptibility of three-dimensional arrays composed from the rings. Our simulation results show that the positive peak of the susceptibility remains Lorentz-like shaped and gradually vanishes when the ring's concentration decreases. The amplitude of the peak is also decreases sharply when the temperature increases.

**2 Theory** To simulate InAs/GaAs nano-objects, we use the effective one-electronic-band Hamiltonian with energy and position dependent electron effective mass and Landé factor [16]:

$$\hat{H} = \frac{1}{2}\boldsymbol{\Pi}_{\mathbf{r}} \frac{1}{m(E,\mathbf{r})} \boldsymbol{\Pi}_{\mathbf{r}} + V(\mathbf{r}) + \frac{\mu_B}{2} g(E,\mathbf{r}) \boldsymbol{\sigma} \cdot \mathbf{B} \quad (7)$$

where $\boldsymbol{\Pi}_{\mathbf{r}} = -i\hbar\nabla_{\mathbf{r}} + e\mathbf{A}(\mathbf{r})$ is the momentum operator, $\nabla_{\mathbf{r}}$ is the spatial gradient, $\mathbf{A}(\mathbf{r})$ is the vector potential of the magnetic field $\mathbf{B} = \text{curl}\mathbf{A}(\mathbf{r})$, $V(\mathbf{r})$ is the electronic confinement potential, $\boldsymbol{\sigma}$ is the vector of the Pauli matrices, $m(E, \mathbf{r})$ is the energy ($E$) and position ($\mathbf{r} = \{x, y, z\}$) dependent electron effective mass:

$$\frac{1}{m(E,\mathbf{r})}=\frac{1}{m(\mathbf{r})}\left[\frac{2}{E_g(\mathbf{r})}+\frac{1}{E_g(\mathbf{r})+\Delta(\mathbf{r})}\right]^{-1}\times\left[\frac{2}{E+E_g(\mathbf{r})-V(\mathbf{r})}+\frac{1}{E+E_g(\mathbf{r})-V(\mathbf{r})+\Delta(\mathbf{r})}\right], \quad (8)$$

$g(E, \mathbf{r})$ is the effective Landé factor:

$$g(E,\mathbf{r})=2-\frac{2m_0}{m(E,\mathbf{r})}\cdot\frac{\Delta(\mathbf{r})}{3[E+E_g(\mathbf{r})-V(\mathbf{r})]+2\Delta(\mathbf{r})}, \quad (9)$$

$m(\mathbf{r})$ is the position dependent effective mass at the bottom of the conducting band, $E_g(\mathbf{r})$ is the position dependent band gap, and $\Delta(\mathbf{r})$ is the position spin-orbit interaction splitting.

Mapping the electronic confinement potential $V(\mathbf{r})$, we simulate the actual strain and In content in the nano-rings embedded in the GaAs matrix. First we define the function $h(x, y)$ which presents the dependence of the height of the ring in $z$-direction (the system's growth direction) on the actual position on $xy$-plane (see Fig. 1). Using structural and composition information obtained from AFM (atomic force microscopy) and XSTM (cross-sectional scanning tunnelling microscopy) measurements, the function $h(x, y)$ can be readily discovered and even analytically approximated for most of the objects. For the InAs/GaAs NRs the experimental data fitting suggest [18, 20, 21]:

$$h_r(x,y)=h_0+\gamma_0^2\frac{[h_M(x,y)-h_0]}{R^2}\cdot\frac{R^2-r(x,y)^2}{r(x,y)^2+\gamma_0^2}, \quad r(x,y)\le 0,$$
$$h_r(x,y)=h_\infty+\gamma_\infty^2\frac{[h_M(x,y)-h_\infty]}{r(x,y)^2+\gamma_\infty^2}, \quad r(x,y)>0, \quad (10)$$

where

$$r(x,y)=\sqrt{x^2+y^2}-R,$$
$$h_M(x,y)=h_{M0}\left(1+\xi\frac{x^2-y^2}{x^2+y^2}\right).$$

$h_0, h_{M0}, h_\infty$ stand correspondingly for the height at the center of the ring, at the rim of the ring (where $r(x, y) = 0$), and far away from the center of the ring; $\gamma_0$, $\gamma_\infty$, respectively determine the inner and outer slope near the rim, and the parameter $\xi$ defines the anisotropy of the ring's height on the $xy$-plane. The electronic confinement potential obviously reflects the ring geometry:

$$V(x,y,z)=\Delta E_C\times\left\{1-\frac{1}{4}\left[1+\tanh\left(\frac{z}{a}\right)\right]\times\left[1-\tanh\left(\frac{z-h(x,y)}{a}\right)\right]\right\} \quad (11)$$

where $\Delta E_C$ is the electronic band offset for InAs/GaAs heterostructures. The slope and range of the potential change at the boundaries of the ring are controlled by the parameter $a$ (the hard wall confinement relates to $a \to 0$). We use the potential (11) to define the mapping function as the following:

$$M(x,y,z)=1-\frac{V(x,y,z)}{\Delta E_C}. \quad (12)$$

The mapping function accumulates all experimental information about geometry (shape) and position dependent composition of the ring. Using $M(x, y, z)$, we model the position dependent band gap $E_g(x, y, z)$, spin–orbit interaction splitting $\Delta(x, y, z)$, and effective mass at the bottom of the conducting band $m(x, y, z)$:

$$E_g(x,y,z)=E_g^{in}M(x,y,z)+E_g^{out}[1-M(x,y,z)],$$
$$\Delta(x,y,z)=\Delta^{in}M(x,y,z)+\Delta^{out}[1-M(x,y,z)], \quad (13)$$
$$m(x,y,z)=m^{in}M(x,y,z)+m^{out}[1-M(x,y,z)],$$

where the subscripts "in" and "out" denote the actual material parameters inside and far outside the ring.

For electrons confined in the nano-ring, the energy eigenstates $E_n$ and corresponding envelop wave functions $F_n(\mathbf{r})$ satisfy the Schrödinger equation

$$\hat{H}F_n(\mathbf{r})=E_nF_n(\mathbf{r}). \quad (14)$$

Now, we use solutions of Eq. (14) with the Hamiltonian (7) to define magnetization (magnetic moment) and DMS of the ring (note: the system should be described as a grand canonical ensemble [11, 19]):

$$M_r(B,T)=-\frac{\partial F}{\partial B}=-\sum_n\frac{\partial E_n(B)}{\partial B}f(E_n-\zeta),$$
$$\chi_r(B,T)=\frac{\partial M_r(B,T)}{\partial B}, \quad (15)$$

where the electrochemical potential $\zeta$ of the Fermi–Dirac distribution $f(E–\zeta)$ is defined by the average number of electrons in the ring $\nu$:

$$\nu=\sum_n f(E_n-\mu). \quad (16)$$

Now, according to the general approach to the integrated magnetic response of three-dimensional arrays of the magnetic dipoles (each of the magnetic polarizability $\chi_r$) we use the Claussius–Mossotti relation [13] to define the effective permeability $\mu_{eff}$ and susceptibility $\chi_{eff}$ of three dimensional arrays composed from the rings:

$$\mu_{eff}=\mu_0\frac{1+\frac{2}{3}\mu_0N\chi_r}{1-\frac{1}{3}\mu_0N\chi_r}=\mu_0(1+\chi_{eff}) \quad (17)$$

or

$$\chi_{\text{eff}} = \frac{\mu_0 N \chi_r}{1 - \frac{1}{3}\mu_0 N \chi_r} \tag{18}$$

where $N$ stands for the concentration of the rings in the arrays.

**3 Simulation results and discussion** We simulate magnetic response of NRs using realistic material parameters for semiconductor InAs/GaAs heterostructures with complex strained compositions. According to Refs. [19–24]: $E_g^{in} = 0.86$ eV, $E_g^{out} = 1.519$ eV, $\Delta_{in} = 0.37$ eV, $\Delta_{out} = 0.341$ eV, $m_{in} = 0.044 m_0$, $m_{out} = 0.067 m_0$, $V_{min} = 0$ eV, $V_{max} = \Delta E_C = 0.474$ eV. Simulating the shape and geometrical parameters of NRs, we also admit experimental data from Refs. [10, 15]. More specifically parameters for $h(x, y)$ are: $h_0 = 1.6$ nm, $h_M = 3.6$ nm, $h_\infty = 0$ nm, $\gamma_0 = 3$ nm, $\gamma_\infty = 5$ nm, $0 \le \xi \le 0.2$, $8.5\text{ nm} \le R \le 11.5$ nm, and $a = 0.5$ nm. The electronic confinement potential calculated for our wobbled nano-ring with $\xi = 0.2$ and $R = 12.5$ nm is presented in Fig. 2 in two projections and it obviously reproduces the system geometry and material content.

The Schrödinger Eq. (14) was solved by the nonlinear iterative method [25, 26] using Comsol Multiphysics package [27]. Then, we used the solutions to simulate the DMS of a single electron wobbled InAs/GaAs nano-ring at $T = 1.2$ K which is shown in Fig. 3. At low temperatures, the single electron DMS has a positive peak near 14T. The actual position of the peak is in a very good agreement with the experiment data from Ref. [15] (for $\xi = 0$ and $R = 8.5$ nm). The peaks results of the crossing of two lowest energy levels (see inset in Fig. 3). With temperature increasing the peak remains Lorentz-like shaped and gradually disappears.

Having ready the DMS of individual nano-rings, we use Eq. (18) to simulate the effective magnetic susceptibility of three-dimensional arrays composed from the rings. Our results show that the positive peak remains for the effective susceptibility of the arrays. The peak is obviously Lorentz-like shaped and gradually vanishes when the ring's concentration decreases (see Fig. 4). The temperature dependence of the effective susceptibility peak amplitude for the arrays of NRs is shown in Fig. 5. The amplitude of the peak also decreases with the temperature increase.

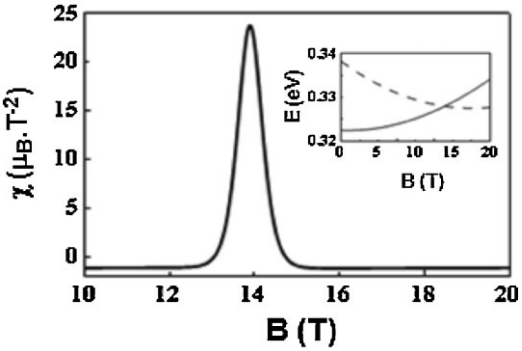


**Figure 3** DMS of the single electron nano-ring as a function on the magnetic field. Inset: Two lowest energy levels for electrons confined in the ring.

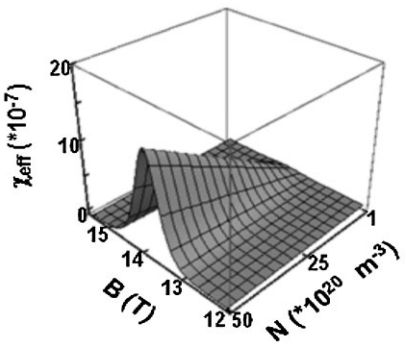


**Figure 4** Effective susceptibility of three-dimensional arrays of nano rings at $T = 1.2$ K.

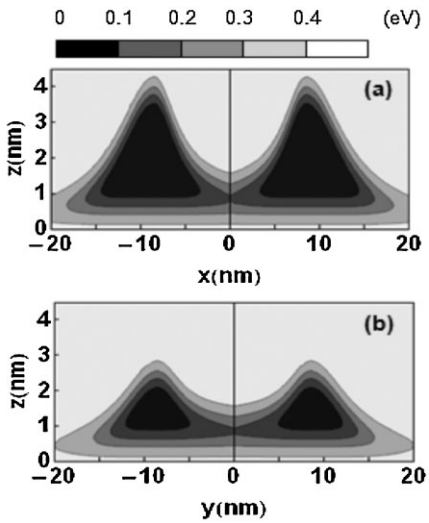


**Figure 2** The electronic confinement potential projected onto: (a) $xy$-plane and (b) $yz$-plane.

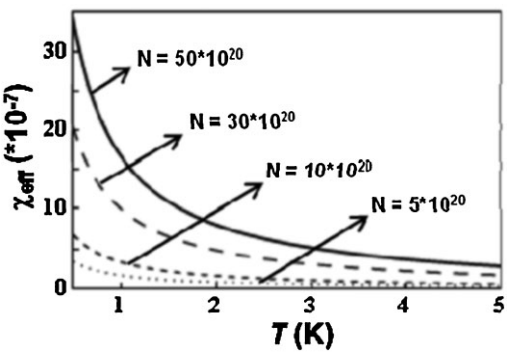


**Figure 5** Temperature dependence of the effective susceptibility peak amplitude for different ring's concentrations.

**4 Conclusions** Using our mapping method, we have built a realistic model of the geometry, structure, and composition of InAs/GaAs wobbled nano-rings. The method allowed us efficiently to simulate magnetic properties of the rings. The simulations were carried out for the three-dimensional model of nano-rings with the smooth electronic confinement potential, effective one band Hamiltonian with position and energy dependent effective mass and $g$-factor. Based on these results, we developed theoretical description of the effective magnetic response of three-dimensional arrays of the rings. Our simulation results demonstrate the "negative"-diamagnetism – the positive effective susceptibility peak – for systems made from conventional diamagnetic materials. The peak remains Lorentz-like shaped and gradually vanishes when the rings' concentration decreases and the temperature increases. It follows from this theoretical study that systems of semiconductor nano-objects can demonstrate very unusual magnetic properties unlike conventional atomic systems. Experimental investigations of the diamagnetic response of arrays of nano-objects made from conventional semiconductors will yield interesting results and can be useful for further fabrication of metamaterials with principally new magnetic properties.

**Acknowledgements** This work is supported by the National Science Council of the Republic of China under Contracts No. 97-2112-M-009-012-MY3, NSC 97-2120-M-009-004, and Vietnam National Foundation for Science and Technology Development (NAFOSTED) under grant number 103.02-2012.05.

## References

[1] D. R. Smith, J. B. Pendry, and M. C. K. Wiltshire, Science **305**, 788 (2004).
[2] S. A. Ramakrishna, Rep. Prog. Phys. **68**, 449 (2005).
[3] W. J. Padilla, D. N. Basov, and D. R. Smith, Mater. Today **9**, 28 (2006).
[4] V. M. Shalaev, Nature Photon. **1**, 41 (2007).
[5] J. Stangl, V. Holý, and G. Bauer, Rev. Mod. Phys. **76**, 725 (2005).
[6] F. Boxberg and J. Tulkki, Rep. Prog. Phys. **70**, 1425 (2007).
[7] R. Hanson, L. P. Kouwenhoven, J. R. Petta, S. Tarucha, and L. M. K. Vandersypen, Rev. Mod. Phys. **79**, 1217 (2007).
[8] J. M. García, G. Medeiros-Ribeiro, K. Schmidt, T. Ngo, J. L. Feng, A. Lorke, J. Kotthaus, and P. M. Petroff, Appl. Phys. Lett. **71**, 2014 (1997).
[9] A. Lorke, R. J. Luyken, A. O. Govorov, J. P. Kotthaus, J. M. Garcia, and P. M. Petroff, Phys. Rev. Lett. **84**, 2223 (2000).
[10] P. Offermans, P. M. Koenraad, J. H. Wolter, D. Granados, J. M. García, V. M. Fomin, V. N. Gladilin, and J. T. Devreese, Appl. Phys. Lett. **87**, 131902 (2005).
[11] L. D. Landau and E. M. Lifshitz, Statistical Physics, Pt. 1 (Pergamon, New York, 1975, ).
[12] J. D. Patterson and B. C. Bailey, Solid-State Physics (Springer, Berlin, 2005).
[13] J. D. Jackson, Classical Electrodynamics (John Wiley and Son Inc., New York, 1998).
[14] Y. Aharonov and D. Bohm, Phys. Rev. **115**, 485 (1959).
[15] N. A. J. M. Kleemans, I. M. A. Bominaar-Silkens, V. M. Fomin, V. N. Gladilin, D. Granados, A. G. Taboada, J. M. García, P. Offermans, U. Zeitler, P. C. M. Christianen, J. C. Maan, J. T. Devreese, and P. M. Koenraad, Phys. Rev. Lett. **99**, 146808 (2007).
[16] O. Voskoboynikov, Y. Li, H. M. Lu, C. F. Shih, and C. P. Lee, Phys. Rev. B **66**, 155306 (2002).
[17] J. I. Climente, J. Planelles, and J. L. Movilla, Phys. Rev. B **70**, 081301 (2004).
[18] V. M. Fomin, V. N. Gladilin, S. N. Klimin, J. T. Devreese, N. A. J. M. Kleemans, and P. M. Koenraad, Phys. Rev. B **76**, 235320 (2007).
[19] O. Voskoboynikov and C. P. Lee, Physica E **20**, 278, (2004).
[20] L. M. Thu and O. Voskoboynikov, Phys. Proc. **3**, 1133 (2010).
[21] L. M. Thu and O. Voskoboynikov, AIP Conf. Proc. **1233**, 952 (2010).
[22] L. M. Thu, W. T. Chiu, and O. Voskoboynikov, Phys. Rev. B **85**, 205419 (2012).
[23] C. E. Pryor and M. E. Pistol, Phys. Rev. B **72**, 205311 (2005).
[24] I. Vurgaman, J. R. Meyer, and L. R. Ram-Mohan, J. Appl. Phys. **89**, 5815 (2001).
[25] Y. M. Li, O. Voskoboynikov, C. P. Lee, and S. M. Sze, Comput. Phys. Commun. **141**, 66 (2001).
[26] M. M. Betcke and H. Voss, Commun. Comput. Phys. **11**, 1591 (2012).
[27] www.comsol.com.

 